Simulating Dark Expressions and Interactions of *frq* and *wc-1* in the *Neurospora* Circadian Clock

Christian I. Hong,*† Ingunn W. Jolma,* Jennifer J. Loros,‡ Jay C. Dunlap,†‡ and Peter Ruoff*
*Department of Mathematics and Natural Science, University of Stavanger, N-4036 Stavanger, Norway; and Departments of †Genetics and ‡Biochemistry, Dartmouth Medical School, Hanover, New Hampshire 03755

ABSTRACT Circadian rhythms are considered to play an essential part in the adaptation of organisms to their environments. The occurrence of circadian oscillations appears to be based on the presence of transcriptional-translational negative feedback loops. In *Neurospora crassa*, the protein FREQUENCY (FRQ) is part of such a negative feedback loop apparently by a direct interaction with its transcription factor WHITE COLLAR-1 (WC-1). Based on the observation that nuclear FRQ levels are significantly lower than nuclear WC-1 levels, it was suggested that FRQ would act more like a catalyst in inhibiting WC-1 rather than binding to WC-1 and making an inactive FRQ:WC-1 complex. Intrigued by this hypothesis, we constructed a model for the *Neurospora* circadian clock, which includes expression of the *frq* and the *wc-1* genes and their possible interactions. The model suggests that even small amounts of nuclear FRQ-protein are capable of inhibiting *frq* transcription in a rhythmic manner by binding to WC-1 and promoting its degradation. Our model predicts the importance of a FRQ dependent degradation of WC-1 in closing the negative feedback loop. The model shows good agreement with experimental levels in nuclear and cytosolic FRQ and WC-1, their phase relationships, and several clock mutant phenotypes.

INTRODUCTION

Circadian oscillators are important in the daily and seasonal adaptation of organisms to their environment (1–4). These oscillators are assumed to act as timing devices (''clocks'') and induce, probably due to measurement of the day length, daily and seasonal processes that are crucial for the organism's environmental adaptation and survival (2).

In many organisms, the circadian oscillator is composed of a transcriptional-translational negative feedback loop of certain clock genes (1,5), which sometimes are also associated with the occurrence of positive feedback loops (6). In the model organism *Neurospora crassa* (7), the transcriptional translational negative feedback loop of the *frequency* (*frq*) gene has been found to be essential for its circadian conidiation rhythm (8,9). The *frq* transcription is activated by the WHITE COLLAR complex (WCC), a heterodimer of the zinc-finger proteins WC-1 and WC-2, where WC-2 is expressed at a constant and abundant level in excess over WC-1 (10–12). The protein FREQUENCY (FRQ) promotes the synthesis of WC-1, leading to a positive feedback (6,13). The negative feedback occurs by the translocation of cytosolic FRQ into the nucleus where FRQ inhibits its own transcription, apparently by interacting with the WCC and with the help of an RNA helicase, the ''FRQ-interacting RNA helicase'', FRH (14). The mechanisms of how FRQ inhibits its own transcription are the object of active research (12,14–16). Recent experiments indicate (16,17) that WC-1 is mainly located in the nucleus, whereas most of FRQ is found in the cytosol. Due to the low amount of nuclear FRQ (FRQ_n) in comparison with WC-1, it was suggested that FRQ could not inhibit the WCC by complex formation. Instead, FRQ was proposed to act more as a catalyst in a phosphorylation-dependent inactivation of WCC (13,16). In this article paper we describe and analyze a kinetic model for circadian oscillations in *N. crassa* under dark conditions. The model predicts that even at low levels, FRQ_n can inhibit *frq* transcription by binding to WCC with a 1:1 stoichiometry. The prerequisite for sustained oscillations is the removal of the FRQ_n:WCC complex from the system, for example by degradation. Our model is the first that highlights the importance of FRQ-dependent degradation of WCC ($WC\text{-}1_n$), which is under investigation. In the case when FRQ_n inhibits the WCC in a catalytic-like manner, oscillations only appear possible when FRQ_n is removed rapidly enough from the system.

THE MODEL

The model is shown in Fig. 1 *A*. Steps 1–6 represent the expression of *frq*, including transcription (step 1), translation (step 2), and translocation of FRQ protein into the nucleus (step 3), the degradation of *frq* mRNA (step 4), as well as degradation of cytosolic and nuclear FRQ (steps 5–6). We considered different rate constants for cytosolic and nuclear FRQ degradation to make minor adjustments in the period for the *frq* mutants. Because there is much less nuclear FRQ than cytoplasmic FRQ, and because the degradation rate constant of nuclear FRQ (k_6) is significantly lower than the cytosolic FRQ degradation rate constant (k_5), in the model the degradation of total FRQ is mostly determined by the cytosolic FRQ degradation. The cytosolic FRQ degradation

Submitted June 14, 2007, and accepted for publication October 15, 2007.

Christian I. Hong and Ingunn W. Jolma contributed equally to this work.

Address reprint requests to Peter Ruoff, University of Stavanger, Faculty of Science and Technology, Dept. of Mathematics and Natural Science, N-4036 Stavanger, Norway. Tel.: 47-5183-1887; Fax: 47-5183-1750; E-mail: peter.ruoff@uis.no.

Editor: Edward H. Egelman.

0006-3495/08/02/1221/12 $2.00

doi: 10.1529/biophysj.107.115154

rate constants are in good agreement with experimental estimates of total FRQ degradation (Table 1; see Ruoff et al. (31)). The results from the model remain similar even when k_5 and k_6 values are set equal to the experimental FRQ degradation rate constants but with slightly shorter periods and reduced amounts of FRQ. Steps 7–12 represent the expression of *wc-1* and nuclear localization of WC-1 with degradation reactions (steps 10–12). WC-2 is present in excess over WC-1 and the concentration of WC-2 does not change during the circadian cycle (11,12). Therefore, we consider WC-2 as a constant and have not included WC-2 in the model. In addition, the WCC complex is represented by WC-1_n. Step 8 describes the FRQ promoted accumulation of WC-1. Several ways to represent step 8 have been investigated and will be discussed below. The step with rate constant k_{02} represents a minor contribution to WC-1_c synthesis in the absence of FRQ (6,11,13). Steps 13–15 represent the inactivation of WC-1_n by binding to FRQ_n with a 1:1 stoichiometry and the subsequent degradation (or inactivation) of the formed complex. Step 16 represents the binding of WC-1_n at the *frq* promoter. The *frq* promoter contains two light responsive elements (LREs), where the distral element (''the clock (C)-box'') (18) appears necessary for rhythmicity (19). Each LRE contains two GATN sequence repeats, each probably capable of binding the Zn-finger domain from either WC-1 or WC-2. In its present form, the model suggests that at least two WC-1_n molecules need to bind to the promoter (C-box), because a reaction order <2 (with respect to $[\text{WC-1}_n]$, see Eq. 1a) does not generate oscillations. With an increasing reaction order/Hill coefficient, ≥ 2 oscillations are more easily generated with a larger oscillatory domain, which was also observed in other studies; see for example Yu et al. (20). The binding of WC-1_n to the *frq* promoter is described as a rapid equilibrium with dissociation constant K leading to Eq. 1a in the *frq* transcription rate; for derivation see Appendix. The rate equations of the model are:

$$\frac{d[frq\,\text{mRNA}]}{dt} = k_1\frac{[\text{WC-1}_n]^2}{K + [\text{WC-1}_n]^2} - k_4[frq\,\text{mRNA}] + k_{01} \tag{1a}$$

$$\frac{d[FRQ_c]}{dt} = k_2[frq\,\text{mRNA}] - (k_3 + k_5)[FRQ_c] \tag{1b}$$

$$\frac{d[FRQ_n]}{dt} = k_3[FRQ_c] + k_{14}[FRQ_n : \text{WC-1}_n] - [FRQ_n](k_6 + k_{13}[\text{WC-1}_n]) \tag{1c}$$

$$\frac{d[wc\text{-}1\,\text{mRNA}]}{dt} = k_7 - k_{10}[wc\text{-}1\,\text{mRNA}] \tag{1d}$$

$$\frac{d[\text{WC-1}_c]}{dt} = \frac{k_8[FRQ_c][wc\text{-}1\,\text{mRNA}]}{K_2 + [FRQ_c]} - (k_9 + k_{11})[\text{WC-1}_c] + k_{02}[wc\text{-}1\,\text{mRNA}] \tag{1e}$$

$$\frac{d[\text{WC-1}_n]}{dt} = k_9[\text{WC-1}_c] - [\text{WC-1}_n](k_{12} + k_{13}[FRQ_n]) + k_{14}[FRQ_n : \text{WC-1}_n] \tag{1f}$$

$$\frac{d[FRQ_n : \text{WC-1}_n]}{dt} = k_{13}[FRQ_n][\text{WC-1}_n] - (k_{14} + k_{15})[FRQ_n : \text{WC-1}_n]. \tag{1g}$$

Concentrations in arbitrary units (a.u.) reflect the number of molecules/moles per cell/septum department. Table 1 shows the rate constants and activation energies for the modeled *frq* alleles and the ER24 mutant. Experimentally determined rate constants are indicated in Table 1 by an asterisk together with respective references. The other rate constants have been chosen to fit the model to experimental observations such as phase relationships among different components and various mutant behaviors. Fig. 1, *B* and *C*, show alternative possibilities for how WC-1_n inactivation can occur, which are discussed later in this article. The rate equations for these additional inhibition mechanisms are given in the Supplementary Material.

TABLE 1 Rate constants (25°C) and activation energies

	frq^+	Frq^1	Frq^7	frq^{S513I}
k_3, h^{-1}	0.05	0.15	0.05	0.05
k_5, h^{-1} (31)*	0.27	0.4	0.15	0.1
K_6, h^{-1}	0.07	0.1	0.01	0.006

Other rate constants (*frq* mutant independent; experimental rate constants are indicated by an asterisk followed by a reference): $k_1 = 1.8$ a.u. h^{-1}; $k_2 = 1.8$ a.u. h^{-1}; $*k_4 = 0.23$ h^{-1} (29); $k_7 = 0.16$ a.u. h^{-1}; $k_8 = 0.8$ a.u. h^{-1}; $k_9 = 40.0$ a.u. h^{-1}; $*k_{10} = 0.1$ h^{-1} (20); $k_{11} = 0.05$ h^{-1}; $k_{12} = 0.02$ h^{-1}; $k_{13} = 50.0$ a.u. h^{-1}; $k_{14} = 1.0$ h^{-1}; $k_{15} = 5.0$ h^{-1}; $K = 1$ .25 a.u (describing frq^+); $K = 8.5$ a.u (describing ER24); $K_2 = 1.0$ a.u.; a.u. = arbitrary units. Activation energies (kJ/mol) for the temperature description of frq^+ and ER24: $E_1 = 62.6$; $E_2 = 20.9$; $E_3 = 25.4$; $E_4 = 15.2$; E_5, curved Arrhenius equation, see Figs. S4 (Supplementary Material); $E_6 = 31.9$; $E_7 = 104$; $E_8 = 22.0$; $E_9 = 66.2$; $E_{10} = 30.0$; $E_{11} = 50.6$; $E_{12} = 25.4$; $E_{13} = 58.6$; $E_{14} = 50.2$; $E_{15} = 50.4$; E_K, curved Arrhenius equation, see Fig. S4 (Supplementary Material); $E_{K_2} = 68.8$.

Computational methods

The differential equations were solved numerically and analyzed by using the FORTRAN subroutine LSODE (21) and XPPAUT (22). Ode-files, FORTRAN code, and a MATLAB (The MathWorks, Natick, MA, www.mathworks.com) version of the model are available.

RESULTS

Modeling frq^+ behavior

Fig. 2 shows the oscillations for the frq^+ parameterization. In Fig. 2 *A*, total (nuclear and cytosolic) amounts of WC-1 and FRQ are shown along with their respective mRNAs. As seen from Eq. 1d, no transcriptional regulation of *wc-1* mRNA is

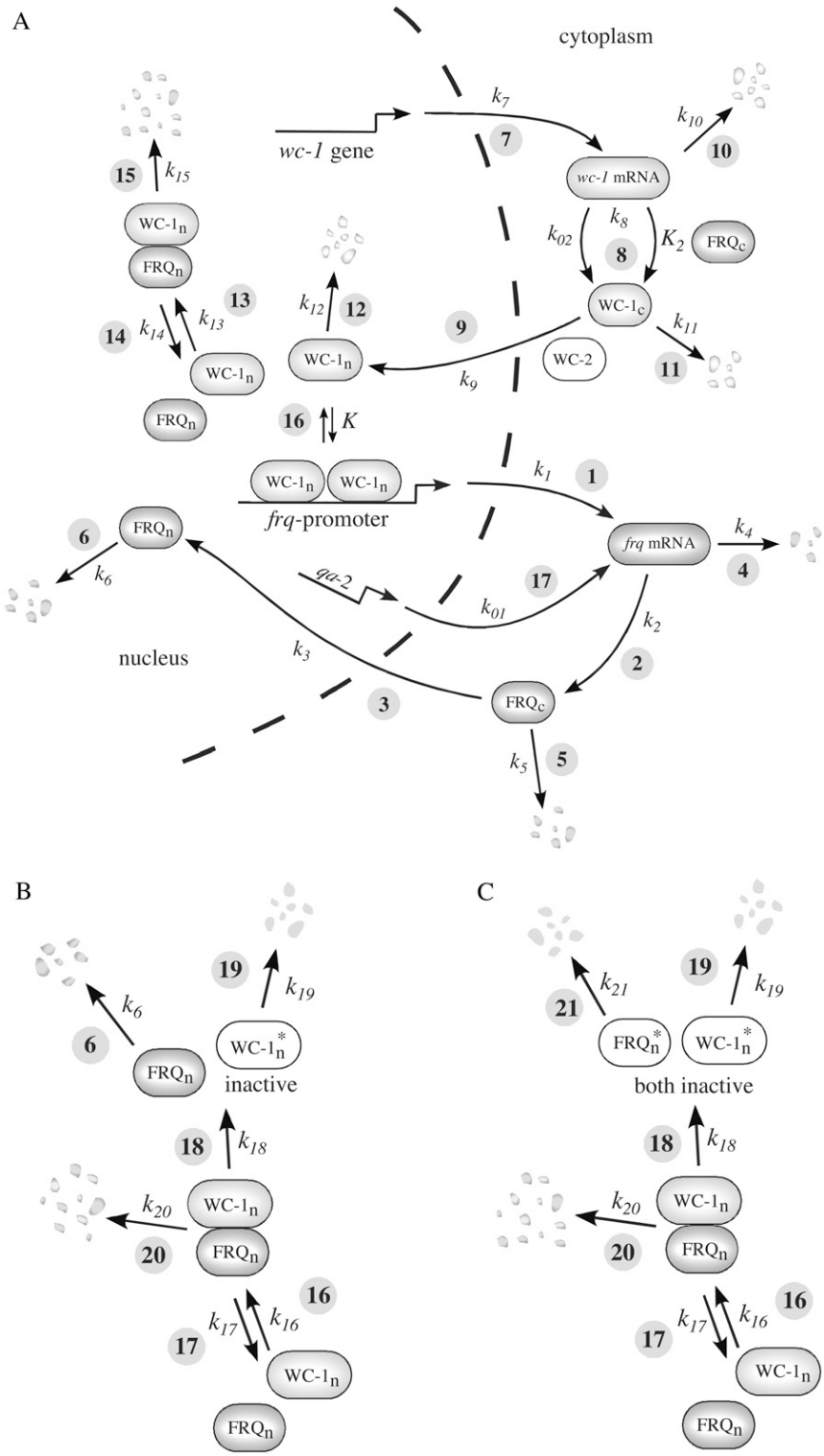

FIGURE 1 Model of the *Neurospora* clock containing different interactions between nuclear FRQ and nuclear WC-1 (representing the WCC). (*A*) Model with FRQ_n:$WC\text{-}1_n$ formation and degradation. This model is described by Eqs. 1a–g. The concentration of WC-2 is constant and not included in the equations. For discussion, see main text and the Appendix. (*B*) Model where FRQ_n inhibits $WC\text{-}1_n$ by a ''catalytic-like'' interaction. (*C*) Model leading to inactive $WC\text{-}1_n^*$ and FRQ_n^*. This model is kinetically equivalent to that shown in Fig. 1 *A*.

considered, leading to a constant *wc-1* mRNA level as observed experimentally (6). Total FRQ and WC-1 oscillations have, as observed experimentally (6), a phase difference of ~7 h (Fig. 2 *A*). As shown by experiments (12,14,16), total FRQ levels are comparable or higher than total WC-1 levels (Fig. 2 *A*), but this situation is reversed in the nucleus where most of the WC-1 is located (16) (Fig. 2 *C*). The reaction rates (time derivative of concentration) in total FRQ and WC-1 levels are predicted to show an ''inverse variation relationship'', i.e., whenever the velocity of total FRQ production (or

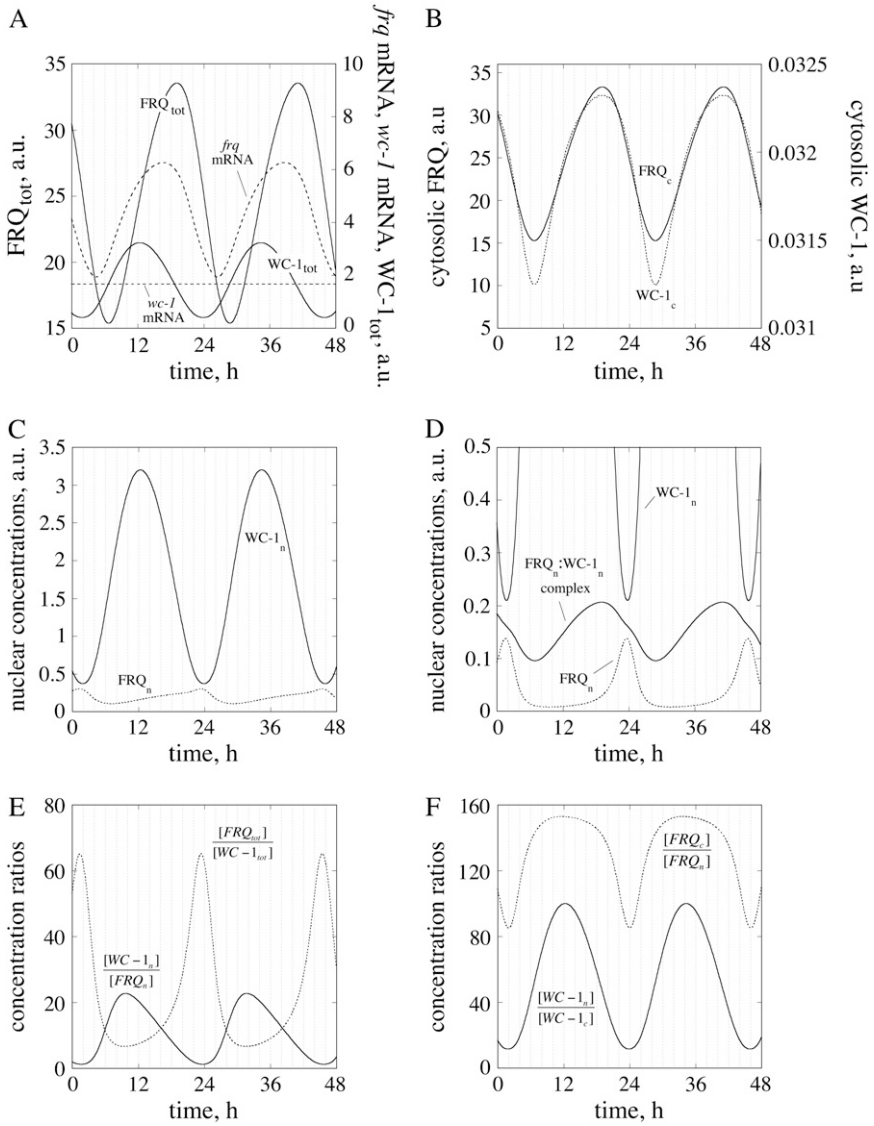

FIGURE 2 Oscillation profiles for frq^{+} parameterization. (*A*) Oscillations in *frq* and *wc-1* mRNA, and in total FRQ and WC-1 levels. (*B*) In-phase oscillations of cytosolic FRQ and WC-1 proteins. (*C*) Anti-phase oscillations of nuclear FRQ and WC-1 proteins. (*D*) Same oscillations as in *C*, but including the oscillatory complex formation between nuclear FRQ and WC-1. (*E*) Oscillations in the ratios between nuclear WC-1/FRQ levels and total FRQ/WC-1 levels, respectively. (*F*) Oscillations in the ratio between nuclear and cytosolic WC-1 levels and nuclear and cytosolic FRQ levels.

consumption) is at a maximum, the rate of total WC-1 is at a minimum and vice versa (Fig. 2 *A*, Fig. S1 (Supplementary Material)). A similar ''inverse'' phase relationship can be seen between sinus and cosinus functions, as for example in a harmonic oscillator. The apparent reason for this, using a rough description, is that the FRQ production rate is dependent on the concentration of the transcription factor WC-1 (mediated via the *frq*-mRNA), whereas FRQ negatively affects the WC-1 reaction rate by removing it. An implication of this inverse relationship is given in the Discussion.

Fig. 2 *D* shows the oscillations of the FRQ_n:$WC\text{-}1_n$ complex in comparison with nuclear (unbound) WC-1 and FRQ (see also Fig. 2 *C*). This low amount of the FRQ_n:$WC\text{-}1_n$ complex is consistent with experimental observations (12,16,17). Fig. 2, *E* and *F*, show oscillatory concentration ratios between $WC\text{-}1_n$ and FRQ_n, FRQ_{tot} and $WC\text{-}1_{tot}$, and between the nuclear and cytosolic forms of WC-1 and FRQ. The model indicates that all ratios vary significantly during the circadian cycle, because the phases of FRQ and WC-1 are quite different.

Variable expression of *frq* and *wc-1*

Aronson et al. (23) overexpressed *frq* by using a quinic acid (QA) inducible system [frq^{+}(*qa*-2pFRQ)] in a wild-type background. Only small variations in the period length were observed at low QA concentrations, whereas rhythmicity was lost at higher concentrations. The same experiment can be simulated using the model by including an additional transcription of *frq* (process 17, Fig. 1 *A*) with rate constant k_{01}. As observed in the experiment (23), increasing k_{01} values show little changes in the period length, which is rather unexpected considering that the period of a limit cycle oscillator is generally affected by parameter changes. However, oscillations stop when k_{01} becomes too large (Fig. 3, *A* and

B), because the system crosses a Hopf bifurcation (24) and enters into a region of a steady state.

Cheng et al. (11) overexpressed *wc-1* in a *wc-1*$^{-}$, *qa*-WC-1 strain. Whereas at low QA concentrations no oscillations were found, rhythmicity was observed at higher QA levels where increased *wc-1* transcription rates show increased amplitudes of WC-1 and FRQ. As found experimentally (16), the amplitude of total FRQ oscillations in the model is higher than the amplitude for total WC-1 (Fig. 2 *A*), but, as observed by Cheng et al. (11), and as seen in Fig. 3 *C*, both amplitudes increase up to a certain level when *wc-1* expression (k_7) is increased. The period is little affected (Fig. 3 *D*, Fig. S2 (Supplementary Material)).

It may be noted that very similar behavior to that shown in Fig. 3, *C* and *D*, can also be observed (data not shown) when the accumulation rate in WC-1_c (Eq. 1e) is made independent of FRQ_c and is only first-order with respect to *wc-1* mRNA, i.e., when Eq. 1e is written in the form:

$$\frac{d[\text{WC-1}_c]}{dt} = k_8[\textit{wc-1}\ \text{mRNA}] - (k_9 + k_{11})[\text{WC-1}_c] + k_{02}[\textit{wc-1}\ \text{mRNA}]. \quad (1e')$$

Another possibility is that $d[\text{WC-1}_c]/dt$ shows saturation kinetics with respect to *wc-1* mRNA and FRQ_c, where Eq. 1e takes the form:

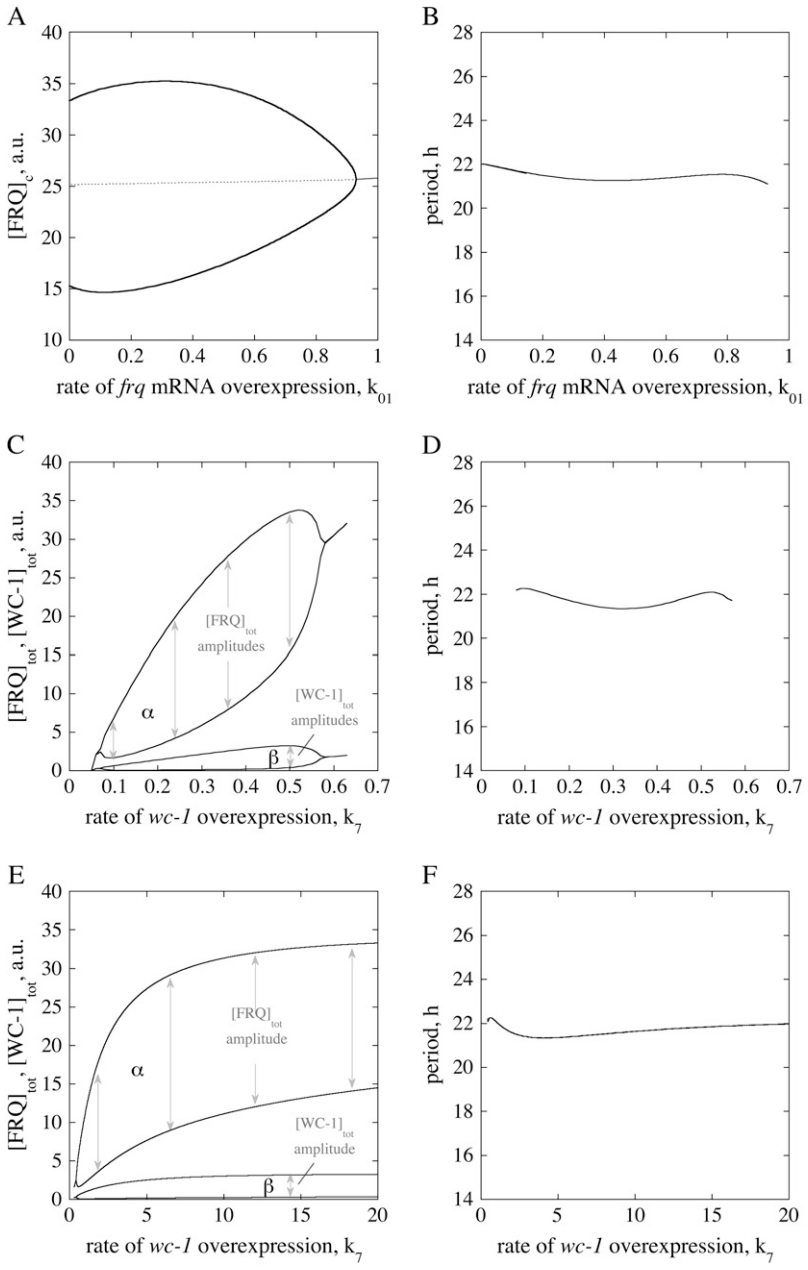

FIGURE 3 Overexpression of *frq* and *wc-1*. (*A*) One-parameter bifurcation diagram of cytosolic FRQ levels as a function of k_{01}. Dashed and solid lines denote the unstable and stable steady states, respectively. (*B*) Period length as a function of k_{01}, simulating the rate of *frq*$^{+}$ (*qa*-2pFRQ) overexpression in a *frq*$^{+}$ genetic background. (*C*) Diagram showing total FRQ and WC-1 levels/amplitudes as a function of *wc-1* transcription rate k_7. (D) Period length as a function of k_7. (*E*) FRQ_{tot} and WC-1_{tot} amplitudes show saturation behavior in *wc-1* overexpression when using Eq. 1e″. (*F*) Period length as a function of k_7 when Eq. 1e″ is used.

$$\frac{d[\text{WC-1}_c]}{dt} = \frac{k_8[FRQ_c]}{K_2 + [FRQ_c]} \times \frac{[wc\text{-}1\ \text{mRNA}]}{K_3 + [wc\text{-}1\ \text{mRNA}]} - (k_9 + k_{11})[\text{WC-1}_c] + k_{02}[wc\text{-}1\ \text{mRNA}]. \quad (1e'')$$

In the case of Eq. 1e″, FRQ_{tot} and $WC\text{-}1_{tot}$ amplitudes (Fig. 3 *E*) and the period length (Fig. 3 *F*) show saturation behavior and become independent of the magnitude of *wc-1* overexpression (k_7), which improves the robustness of the model. A mechanism of how saturation kinetics in FRQ_c and *wc-1* mRNA may occur without saturating protein synthesis kinetics with respect to the ribosomes is discussed below.

Lee et al. (6) applied a 4 h QA pulse in a frq^{10}:*qa*-2FRQ strain and observed that FRQ peaked before WC-1 by ~8–12 h. The model shows the same dynamic behavior as observed in the experiment (Fig. S3, Supplementary Material).

Modeling ER24 mutant behavior

A sufficiently strong binding of WC-1 at the *frq* promoter is needed to get sustained oscillations. Weakening the binding of WC-1 to the *frq* promoter by increasing the dissociation constant *K* (Fig. 1 *A*, Eq. 1a) leads to an increased period and eventually to damped oscillations (*solid lines* in Fig. 4 *A*). A very similar behavior is observed for the mutant ER24. ER24 has an L to I point mutation at a conserved position in the Zn finger DNA-binding domain of WC-2 (25). Thus, the model suggests that ER24 may have a weaker binding of WCC (represented by $WC\text{-}1_n$) to the *frq* promoter.

An interesting aspect of ER24 is its partial loss in temperature compensation with period variations between 23 and 30 h and a period maximum at ~22°C (Fig. 4 *B*). frq^+ shows a similar maximum, but due to its temperature compensation, the period length varies only between 20 h and 22 h (Fig. 4 *B*). We wondered how the model would ''explain'' the concave experimental period-temperature relationship for frq^+ and ER24. Starting with ER24, the model suggests that the dissociation constant *K* is relatively large and increases with increasing temperature (i.e., from 3 to 11 a.u. between 20° and 30°C; Fig. S4A, Supplementary Material), but with a lower activation energy at 30°C compared to 20°C (Fig. S4B, Supplementary Material). For frq^+, the behavior is qualitatively similar, with a strong $WC\text{-}1_n$ binding at 20°C ($K \approx 10^{-3}$ a.u.), which weakens for higher temperatures (>24°C) with *K* values between 1 a.u. and 2 a.u. (Figs. S4C and S4D, Supplementary Material). In addition to these observations, k_5 needs to increase with increasing temperature, but with a curved Arrhenius-plot with apparent activation energies of ~25 kJ/mol for the range 20–25°C and 6 kJ/mol for the range 25–30°C (Figs. S4E and S4F, Supplementary Material).

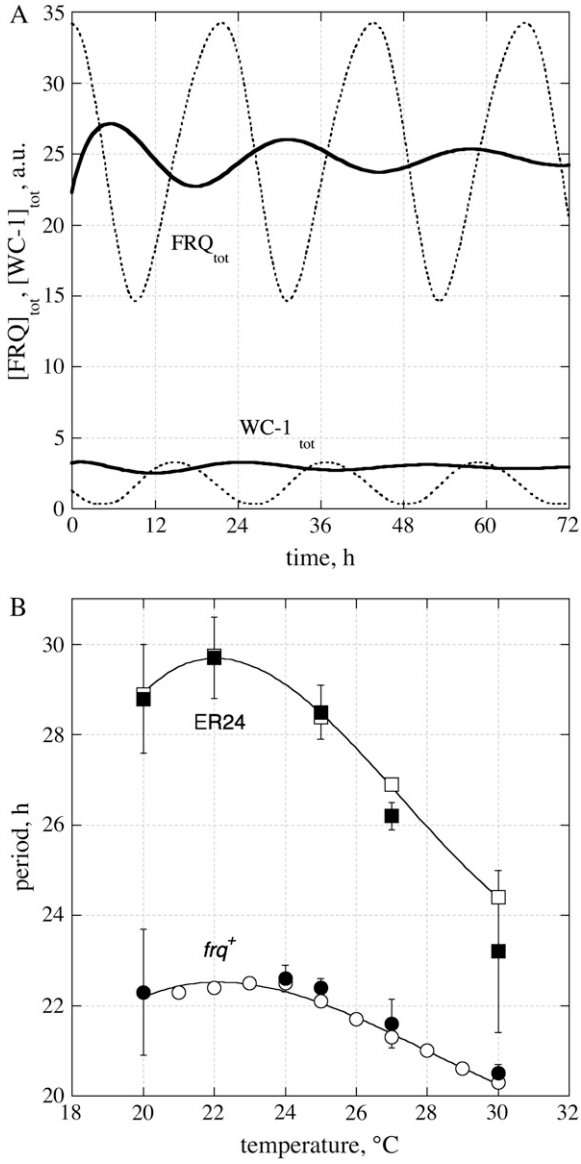

FIGURE 4 Modeling ER24 behavior. (*A*) Oscillations at 25°C describing ER24 behavior (*solid lines*) when *K* is increased from 1.25 a.u. (frq^+ value) to 8.5 a.u. Dotted lines show the frq^+ oscillations. (*B*) Comparison between experimental (*solid symbols*) and simulations (*open symbols*) of temperature behavior for ER24 (*squares*) and frq^+ (*circles*).

Modeling *frq* mutants

Several point mutations in *frq* show altered period lengths (26,27). Calculations (28,29) as well as experiments (30,31) indicate that a high stability of FRQ (slow FRQ degradation such as in frq^7 and frq^{S513I}) leads to large period lengths, whereas a low stability in FRQ (rapid FRQ degradation, such as in frq^1) leads to short periods. The period lengths of frq^1, frq^7, and frq^{S513I} can be modeled using the rate constants shown in Table 1, where the cytosolic FRQ degradation rate constants are in good agreement with experimental estimates (31). For frq^1, a somewhat larger FRQ^1 translocation into the

nucleus had to be assumed to obtain stable oscillations with a period of 16 h. This could be related to the fact that the mutation in frq^1 is close to the nuclear localization sequence of FRQ (26). The model predicts that total FRQ levels are always higher than total WC-1 levels and that FRQ_{tot} oscillations are larger in amplitude than $WC\text{-}1_{tot}$ oscillations, especially for the long-period mutants, which have a higher FRQ protein stability (Fig. S5, Supplementary Material). Nuclear FRQ (FRQ_n) levels are predicted to increase relative to nuclear WC-1 levels with increasing FRQ stability and period (Fig. 5). Whereas in frq^1 and frq^+ nuclear FRQ levels are lower than nuclear WC-1 levels (Fig. 5, *A* and *B*), FRQ_n and $WC\text{-}1_n$ concentrations are approximately equal in frq^7 (Fig. 5 *C*). In frq^{S513I}, the model predicts that nuclear FRQ levels should be significantly larger than $WC\text{-}1_n$ levels (Fig. 5 *D*).

DISCUSSION

Oscillatory behavior

We focus on frq^+ oscillatory behavior because most experiments on relative component concentrations, their amplitudes, and phase relationships have been reported for frq^+. As observed experimentally (12,14,16), the model shows total FRQ levels that are generally larger than total WC-1 levels, whereas nuclear FRQ levels are significantly lower than nuclear WC-1 (Fig. 2 *A*). The amplitude of total FRQ can be characterized as the ratio between maximum and minimum levels of total FRQ. With the parameter set presented here, this ratio is ~2.3, but increases with increasing *wc-1* transcription rates as shown in Fig. 3 *C*. An analysis of published experimental FRQ oscillations shows a considerable variation in this ratio, ranging from ~1.6 to 5 (6,11,32,33). Also the shape (more pulsatile versus more smooth behavior) of the *frq*-mRNA and FRQ oscillations shows considerable variations between experiments. The reason for this variability may have multiple reasons, for example reflecting different types and properties of FRQ antibodies, age of culture, as well as slightly different light or nutritional conditions. As implicitly indicated by the study of Cheng et al. (11), the variability in FRQ amplitude may perhaps also be due to environmental variations in the *wc-1* transcription rate.

The observation that FRQ_n is significantly lower than $WC\text{-}1_n$ levels led to the suggestion (16) that nuclear FRQ may not to be capable of controlling *frq* transcription by binding to the much more abundant $WC\text{-}1_n$. However, the calculations presented here clearly show that even low levels of FRQ_n enable rhythmic *frq* transcription by binding to $WC\text{-}1_n$. The model simulates that the FRQ_n:$WC\text{-}1_n$ complex is present at low concentrations (as found experimentally (16)).

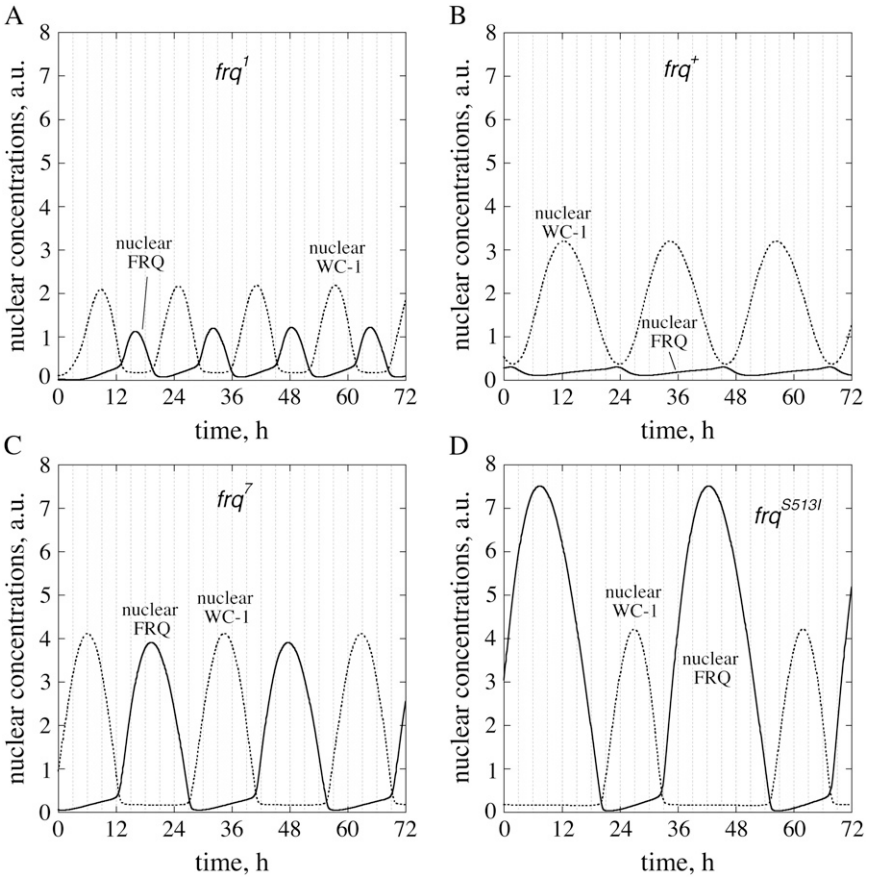

FIGURE 5 Nuclear FRQ levels (*solid lines*) and nuclear WC-1 levels (*dotted lines*) in parameterizations of (*A*) frq^1, (*B*) frq^+, (*C*) frq^7, and (*D*) frq^{S513I}, respectively.

It was recently suggested that FRQ_n may promote, in a ''catalyst-like'' manner, the deactivation of WCC by phosphorylation (13,16). We have investigated this possibility using the scheme shown in Fig. 1 *B*, where FRQ_n interacts with WCC ($WC\text{-}1_n$) and inactivates it by reaction 19. This mechanism was not able to generate oscillations within a 24 h period regime without removing the FRQ_n:$WC\text{-}1_n$ complex (Fig. 1 *B*, reaction 20) and without a significant removal of FRQ_n (reaction 6). However, even when oscillations within the circadian period regime were obtained by allowing FRQ_n and FRQ_n:$WC\text{-}1_n$ removal, the calculated phase difference between FRQ_{tot} and $WC\text{-}1_{tot}$ was too small compared with the experimental (6) and calculated results (Fig. 6). This indicates that the removal of the FRQ_n:$WC\text{-}1_n$ complex appears essential to obtain correctly phased FRQ and WC-1 oscillations, and that a significant amount of FRQ and WC-1 are removed through the FRQ_n:$WC\text{-}1_n$ complex. The mechanism shown in Fig. 1 *C* is kinetically equivalent to the FRQ_n:$WC\text{-}1_n$ degradation mechanism of Fig. 1 *A*, leading to ''inactive'' FRQ_n^* and $WC\text{-}1_n^*$ proteins, which, in principle, may still be detectable by Western blotting. Thus, Western analysis may not be able to distinguish unequivocally between degradation and inhibition mechanisms. A recent model study of the *Neurospora* clock (20) independently indicated that inactivation of $WC\text{-}1_n$ by binding between FRQ and $WC\text{-}1_n$ is more effective than a catalytic inactivation of $WC\text{-}1_n$ by FRQ.

Our model's simulation that *wc-1* mRNA levels do not need to be oscillatory and that the amplitude of $WC\text{-}1_{tot}$ is lower than for FRQ_{tot} (Fig. 1 *A*) is in agreement with experimental findings ((6,34). Furthermore, reaction rates in FRQ_{tot} and $WC\text{-}1_{tot}$ show an ''inverse'' relationship: whenever the (synthesis or degradation) rate in FRQ_{tot} is highest, $WC\text{-}1_{tot}$ levels and $WC\text{-}1_{tot}$ synthesis/consumption rates are approximately constant (Fig. 1 *A*, Fig. S1 (Supplementary Material)). For example, during the decay phase of FRQ_{tot}, the model predicts that $WC\text{-}1_{tot}$ levels remain approximately constant, a behavior that has also been observed experimentally (see Fig. 3 *B* in Schafmeier et al. (13)).

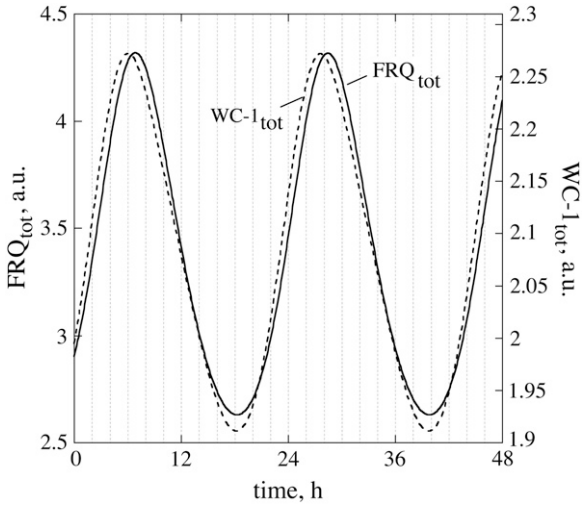

FIGURE 6 Obtained oscillations with a period of 21.6 h using the scheme of Fig. 1 *B* ($k_{13} = k_{14} = k_{15} = 0$) with $k_6 = 1.2\ h^{-1}$, $k_{16} = 50.0$ a.u. h^{-1}, $k_{17} = 0$, $k_{18} = 1.0$ a.u. h^{-1}, $k_{19} = 1.0$ a.u. h^{-1}, and $k_{20} = 3.0 \times 10^{-2}$ a.u. h^{-1}. Note the small difference in phase between FRQ_{tot} and $WC\text{-}1_{tot}$ compared to Fig. 2 *A* and experimental values (6). To get oscillations with a circadian period when using this scheme, the k_6 value needs to be unrealistically high (1.2 h^{-1}) in comparison with experimental results (30–32).

Overexpressing *frq* with the inducible *qa-2* promoter in a frq^+ genetic background shows, in agreement with experiments (23), oscillations with little variation in period (Fig. 3 *A*). When the rate of *frq* overexpression becomes too high, the oscillations stop (crossing a Hopf bifurcation) and the system enters a stable steady-state region (Fig. 3 *B*).

When *wc-1* is overexpressed, the amplitude in total FRQ levels increases with increasing *wc-1* transcription (k_7) rates (Fig. 3, *C* and *E*), whereas only small variations in the period lengths are observed (Fig. 3, *D* and *F*), a behavior that is also found experimentally (11). It is not established (11) whether the *Neurospora* rhythm can show saturation kinetics when *wc-1* is overexpressed as shown in Fig. 3 *E*. However, we wish to point out that robust oscillations showing saturation kinetics in period and amplitudes with respect to *wc-1* overexpression (and without saturating the ribosomes) may occur due to a FRQ-promoted expression of $WC\text{-}1_c$. When the rate of translation is (for the sake of simplicity) first-order with respect to an association between *wc-1* mRNA and FRQ_c, then it can be shown (see Appendix) that overexpression of *wc-1* (increase of k_7) shows saturation kinetics. In this respect, the FRQ-promoted synthesis of $WC\text{-}1_c$ may be a mechanism leading to robust oscillations. The above mechanism is supported by experimental results showing that the FRQ-promoted accumulation of WC-1 needs the presence of WC-2 (13) and that FRQ interacts with WC-2 (12). The reaction sequences 8 and 9 (Fig. 1 *A*) may also be viewed as a FRQ-promoted assembly of WCC as suggested by Schafmeier et al. (13). In summary, and as seen in Fig. 3, *C* and *E*, the model shows (in agreement with experiments (6,11,13)), that FRQ_{tot} oscillations have larger amplitudes than $WC\text{-}1_{tot}$ oscillations.

In agreement with experimental results (28,31), the *frq* mutants are characterized by different FRQ stabilities (Table 1); i.e., in the short-period mutant frq^1, FRQ is more rapidly degraded than in frq^+, whereas in the long-period alleles (frq^7, frq^{S513I}) FRQ is more stable than in frq^+ and the FRQ amplitude increases with increasing FRQ stability (Fig. 5, Fig. S2 (Supplementary Material)). In frq^1, FRQ_n is somewhat higher than in frq^+ (Fig. 5), which is due to the increased import (larger k_3) of FRQ^1 into the nucleus (Table 1).

WC-1 binding to *frq* promoter and temperature compensation

The model predicts that with a decreasing binding strength of $WC\text{-}1_n$ (WCC) to the *frq* promoter, the period increases and oscillations become damped and stop if the dissociation

constant K becomes too large (Fig. 4 *A*), similar to what was observed in ER24 (25). This suggests that in ER24, the binding of WC-1_n to the *frq* promoter should be weaker than in frq^+, especially at low temperatures.

An interesting aspect is that when the binding between WC-1_n and the *frq* promoter weakens (described by increased K values) with increasing temperature, the oscillator can show partial temperature overcompensation at low temperatures as found experimentally. Recently, Daniel Forger from the University of Michigan made the interesting observation that the Goodwin oscillator (35,36) cannot be temperature compensated when its inhibition term K is set to zero (D. Forger, University of Michigan, personal communication, 2006). Because K in the Goodwin oscillator and in the our model reflects a dissociation constant, the model's behavior described in Fig. 4 *C* and the observation by Forger indicate that binding of the transcription factor to the clock protein promoter is part of the temperature compensation mechanism in *Neurospora crassa* and possibly also in other organisms. Clock protein degradation and binding properties at clock protein promoters are some of the processes that are expected to lead to temperature compensation. It will be interesting to see what other processes will be found in the temperature compensation mechanism.

In our model, the temperature dependence for most rate constants is described by a single Arrhenius equation (Table 1). However, to get a close description of the experimental period-temperature profiles for of frq^+ and ER24, a curved Arrhenius plot had to be employed for K and k_5. For k_5, the activation energy values used in the calculations are close to those estimated previously for the range 20–25°C (31), but a significant lower value had to be used ($\approx$ 6 kJ/mol) for the range 25–30°C, where currently no experimental estimate exists. The need for curved Arrhenius plots in describing the temperature dependencies of k_5 and K is not unexpected, because FRQ degradation through the proteasome (37) and the binding of transcription factors to a promoter (38) are complex processes involving a variety of enzymes, proteins, and reaction steps. For example, enzyme- and ribozyme-catalyzed processes (39–42) can show curved or discontinuous Arrhenius plots similar to those shown in Fig. S4 (Supplementary Material). The origin of these curved Arrhenius plots may be related to temperature-induced conformational changes of an enzyme or ribozyme (40) or may already be inherent in the kinetics (40).

Researchers are beginning to unravel the mechanisms contributing to temperature compensation. A balance equation (43) was recently formulated, which is closely related to the concept of opposing reactions made by Hastings and Sweeney in 1957 (44). The balance equation has been able to account for temperature compensation in several chemical (43,45–50) and circadian oscillators (31,36,51–54) and was also applied to steady-state kinetics (55). Our study indicates that the activation energies participating in the balance equation may not necessarily be independent of temperature (as described above) but may result in ''dynamic temperature compensation'' (55) when lumping complex biochemical processes (elementary reactions) into one reaction step. A more detailed analysis of such behavior is being considered elsewhere. There are several other descriptions on how to explain temperature compensation, and the reader is referred to these articles (44,56–61) and references therein.

Comparisons with other models

A variety of models have been put forward to understand the mechanism of the *Neurospora* circadian oscillator focusing on aspects such as single negative feedback loops (36,62–65), interlocking positive and negative feedback loops (20,66,67), delay kinetics (67,68), or the explicit inclusion of the transcription factors WC-1/WCC (20,64,65). The models by Yu et al. (20), Smolen et al. (69), and the (two-loop) models by Francois (67) have included inhibition of WCC by binding of FRQ to WCC with a subsequent degradation of the FRQ-WCC complex. In these models, total FRQ and WCC show anti-phase oscillations as observed in Fig. 2 *C*. Because we were interested whether small amounts of nuclear FRQ would allow the inhibition of WC-1 and lead to realistic oscillatory behavior, our model differs from those of Yu et al. (20), Smolen et al. (69) and Francois (67) by considering explicitly nuclear and cytosolic FRQ and WC-1 levels. In doing so, our model predicts significant phase differences when comparing nuclear FRQ and WC-1 levels (Fig. 2, *C* and *D*) with cytosolic FRQ and WC-1 levels (Fig. 2 *B*). We are also able to describe experimental behavior when overexpressing *frq* and *wc-1* (Fig. 3), and suggest the importance of WC-1_n (WCC) binding to the *frq* promoter as part of *Neurospora's* temperature compensation mechanism (Fig. 4).

SUMMARY

Our model suggests that small amounts of FRQ_n are capable of inhibiting *frq* transcription by binding to WC-1_n (representing WCC) as long as FRQ_n is rapidly degraded or otherwise removed or inactivated together with the interacting WC-1_n. The formed complex between WC-1_n and FRQ_n is present at low oscillatory concentrations compared with WC-1_n. For frq^+, the model is in qualitative agreement with experimental nuclear and cytosolic FRQ and WC-1 levels and their phase relationships and can account for the increase of FRQ amplitude when *wc-1* is overexpressed. The model also accounts for the loss of rhythmicity above a certain level of *frq* overexpression. The model predicts that FRQ levels increase in *frq* mutants in the order $frq^1 < frq^+ < frq^7 < frq^{S513I}$, whereas WC-1 amplitudes in these mutants remain more or less unaffected. The ER24 phenotype can be explained by a weaker WC-1_n (WCC) binding to the *frq* promoter. The observed temperature overcompensation in ER24 and frq^+ can be modeled by an increase of the WC-1_n dissociation from the *frq* promoter with increasing temperatures. The model

suggests that the WC-1_n (WCC) binding to the *frq* promoter is part of *Neurospora's* mechanism for temperature compensation.

APPENDIX

Calculating the rate of *frq* transcription

The *frq* promoter region contains two binding regions for WCC (19), one of which (the clock box or C-box) (18) is required for rhythmicity. The C-box in turn contains two imperfect distinct repeats of a 15 basepair consensus sequence, suggesting that WCC (WC-1_n) binding may occur at two sites. In the following, we use WC-1_n to denote nuclear WCC concentrations:

$$(\text{WC-1}_\text{n})_2 \cdot frq_{\text{promoter}} \rightleftarrows 2\text{WC-1}_\text{n} + frq_{\text{promoter}}. \quad \text{(A1)}$$

Assuming that reaction A1 is in a rapid equilibrium, the equilibrium (i.e., dissociation) constant of reaction A1 is given by:

$$K = \frac{[\text{WC-1}_\text{n}]^2[frq_{\text{promoter}}]}{[(\text{WC-1}_\text{n})_2 \cdot frq_{\text{promoter}}]}. \quad \text{(A2)}$$

The rate of *frq* transcription v is given by Eq. A3:

$$v = k[(\text{WC-1}_\text{n})_2 \cdot frq_{\text{promoter}}]. \quad \text{(A3)}$$

In the model, we assume that the total amount of *frq* promoter regions $[frq_{\text{promoter}}]_{\text{tot}}$ is constant, i.e.,

$$[frq_{\text{promoter}}]_{\text{tot}} = [(\text{WC-1}_\text{n})_2 \cdot frq_{\text{promoter}}] + [frq_{\text{promoter}}]. \quad \text{(A4)}$$

From Eq. A2, an expression for $[frq_{\text{promoter}}]$ can be found and inserted into Eq. A4, giving

$$[frq_{\text{promoter}}]_{\text{tot}} = [(\text{WC-1}_\text{n})_2 \cdot frq_{\text{promoter}}]\left(1 + \frac{K}{[\text{WC-1}_\text{n}]^2}\right). \quad \text{(A5)}$$

Solving Eq. A5 for $[(\text{WC-1}_\text{n})_2 \cdot frq_{\text{promoter}}]$ and inserting it into Eq. A3, leads to the final expression for the rate of *frq* transcription v:

$$v = \frac{k[frq_{\text{promoter}}]_{\text{tot}}[\text{WC-1}_\text{n}]^2}{K + [\text{WC-1}_\text{n}]^2} = \frac{k_1[\text{WC-1}_\text{n}]^2}{K + [\text{WC-1}_\text{n}]^2}, \quad \text{(A6)}$$

with $k_1 = k\,[frq_{\text{promoter}}]_{\text{tot}}$.

Possible saturation kinetics of *wc-1* overexpression

Because FRQ_c and WC-2 are necessary for the expression of WC-1_c (13) and because FRQ and WC-2 interact with each other, we consider that FRQ_c is associated with WC-2. To show saturation behavior in period length and amplitudes when *wc-1* is overexpressed, an interaction between FRQ_c:WC-2 and the translation machinery or *wc-1* mRNA appears necessary. We consider here the interactions between FRQ_c:WC-2 and *wc-1* mRNA, which is assumed to be in rapid equilibrium with the complex FRQ_c:WC-2:*wc-1* mRNA that leads to the translation of *wc-1* mRNA and to a FRQ-assisted formation of WC-1_c:WC-2, i.e.,

$$\text{FRQ}_\text{c}:\text{WC-2} + \textit{wc-1}\ \text{mRNA} \rightleftarrows \text{FRQ}_\text{c}:\text{WC-2}:\textit{wc-1}\ \text{mRNA} \quad \text{(A7)}$$

$$\text{FRQ}_\text{c}:\text{WC-2}:\textit{wc-1}\ \text{mRNA} \xrightarrow{\text{ribosome}} \text{WC-1}_\text{c}:\text{WC-2} + \text{FRQ}_\text{c}. \quad \text{(A8)}$$

The WC-1_c:WC-2 complex is then transported into the nucleus (Fig. 1 *A*).

Because we have not explicitly considered WC-2 in the model equations (the WC-2 concentration is approximately constant and in excess over WC-1 (11)), we do not include WC-2 in the following mass balance equations. If, for a given circadian time,

$$[\text{FRQ}_\text{c}]_{\text{tot}} = [\text{FRQ}_\text{c}] + [FRQ_\text{c}:\textit{wc-1}\ \text{mRNA}] \quad \text{(A9)}$$

$$[\textit{wc-1}\ \text{mRNA}]_{\text{tot}} = [\textit{wc-1}\ \text{mRNA}] + [\text{FRQ}_\text{c}:\textit{wc}-\textit{1}\ \text{mRNA}] \quad \text{(A10)}$$

denote total concentrations of FRQ_c and wc-1 mRNA and $c_0 = [\text{FRQ}_\text{c}]_{\text{tot}} + [\textit{wc-1}\ \text{mRNA}]_{\text{tot}}$, then we can write

$$\begin{aligned} c_0 &= [FRQ_\text{c}] + [\textit{wc-1 mRNA}] + 2[FRQ_\text{c}:\textit{wc-1}\ \text{mRNA}] \\ &= [FRQ_\text{c}:\textit{wc-1 mRNA}]\left(2 + \frac{K_2}{[FRQ_\text{c}]} + \frac{K_2}{[\textit{wc-1}\ \text{mRNA}]}\right), \end{aligned} \quad \text{(A11)}$$

where K_2 is the rapid equilibrium constant between FRQ_c:*wc-1* mRNA, and FRQ_c, *wc-1* mRNA, given by

$$K_2 = \frac{[FRQ_\text{c}][\textit{wc-1}\ \text{mRNA}]}{[FRQ_\text{c}:\textit{wc-1}\ \text{mRNA}]}. \quad \text{(A12)}$$

Because the rate of *wc-1* translation (v_{tr}) is assumed to be proportional to [FRQ_c:*wc-1* mRNA], v_{tr} is proportional to $c_0/(2+K_2/[FRQ_\text{c}]+K_2/[\textit{wc-1}\ \text{mRNA}])$ showing saturation behavior both in FRQ_c or *wc-1* mRNA. As a result, whenever *wc-1* mRNA is overexpressed, its translation rate v_{tr} is limited by the amount of FRQ_c.

SUPPLEMENTARY MATERIAL

To view all of the supplemental files associated with this article, visit www.biophysj.org.

This work was supported by project 169283 from the Leiv Eiriksson mobility program (C.I.H.) and Research Council of Norway grant 1670897/v40 (I.W.J.) to the University of Stavanger, the National Academies Keck Futures Initiative Signaling Grant (C.I.H.), grants from the National Institutes of Health (MH44651 to J.C.D. and J.J.L., R37 GM34985 to J.C.D.), and the core grant to the Norris Cotton Cancer Center at Dartmouth Medical School.

REFERENCES

1. Dunlap, J. C. 1999. Molecular bases for circadian clocks. *Cell.* 96: 271–290. doi:10.1016/S0092-8674(00)80566-8.
2. Bünning, E. 1963. The Physiological Clock. Springer-Verlag, Berlin.
3. Edmunds, L. N. 1988. Cellular and Molecular Bases of Biological Clocks. Springer-Verlag, New York.
4. Dunlap, J. C., J. J. Loros, and P. J. DeCoursey, editors. 2004. Biological Timekeeping. Sinauer Associates, Sunderland, MA.
5. Dunlap, J. C. 1998. Common threads in eukaryotic circadian systems. *Curr. Opin. Genet. Dev.* 8:400–406. doi:10.1016/S0959-437X(98)80109-3.
6. Lee, K., J. J. Loros, and J. C. Dunlap. 2000. Interconnected feedback loops in the *Neurospora* circadian system. *Science.* 289:107–110. doi:10.1126/science.289.5476.107.

7. Davis, R. H. 2000. Neurospora. Contributions of a Model Organism. Oxford University Press, New York.
8. Dunlap, J. C., and J. J. Loros. 2004. The *Neurospora* circadian system. *J. Biol. Rhythms.* 19:414–424. doi:10.1177/0748730404269116.
9. Liu, Y., and D. Bell-Pedersen. 2006. Circadian rhythms in *Neurospora crassa* and other filamentous fungi. *Eukaryot. Cell.* 5:1184–1193. doi:10.1128/EC.00133-06.
10. Crosthwaite, S. K., J. C. Dunlap, and J. J. Loros. 1997. *Neurospora wc-1* and *wc-2*: transcription, photoresponses, and the origins of circadian rhythmicity. *Science.* 276:763–769. doi:10.1126/science.276.5313.763.
11. Cheng, P., Y. Yang, and Y. Liu. 2001. Interlocked feedback loops contribute to the robustness of the *Neurospora* circadian clock. *Proc. Natl. Acad. Sci. USA.* 98:7408–7413. doi:10.1073/pnas.121170298.
12. Denault, D. L., J. J. Loros, and J. C. Dunlap. 2001. WC-2 mediates WC-1-FRQ interaction within the PAS protein-linked circadian feedback loop of *Neurospora*. *EMBO J.* 20:109–117. doi:10.1093/emboj/20.1.109.
13. Schafmeier, T., K. Kaldi, A. Diernfellner, C. Mohr, and M. Brunner. 2006. Phosphorylation-dependent maturation of *Neurospora* circadian clock protein from a nuclear repressor toward a cytoplasmic activator. *Genes Dev.* 20:297–306. doi:10.1101/gad.360906.
14. Cheng, P., Q. He, L. Wang, and Y. Liu. 2005. Regulation of the *Neurospora* circadian clock by an RNA helicase. *Genes Dev.* 19:234–241. doi:10.1101/gad.1266805.
15. He, Q., P. Cheng, Y. Yang, L. Wang, K. H. Gardner, and Y. Liu. 2002. *White collar-1*, a DNA binding transcription factor and a light sensor. *Science.* 297:840–843. doi:10.1126/science.1072795.
16. Schafmeier, T., A. Haase, K. Kaldi, J. Scholz, M. Fuchs, and M. Brunner. 2005. Transcriptional feedback of *Neurospora* circadian clock gene by phosphorylation-dependent inactivation of its transcription factor. *Cell.* 122:235–246. doi:10.1016/j.cell.2005.05.032.
17. Cheng, P., Y. Yang, C. Heintzen, and Y. Liu. 2001. Coiled-coil domain-mediated FRQ-FRQ interaction is essential for its circadian clock function in *Neurospora*. *EMBO J.* 20:101–108. doi:10.1093/emboj/20.1.101.
18. Froehlich, A. C., J. J. Loros, and J. C. Dunlap. 2003. Rhythmic binding of a WHITE COLLAR-containing complex to the frequency promoter is inhibited by FREQUENCY. *Proc. Natl. Acad. Sci. USA.* 100:5914–5919. doi:10.1073/pnas.1030057100.
19. Froehlich, A. C., Y. Liu, J. J. Loros, and J. C. Dunlap. 2002. White Collar-1, a circadian blue light photoreceptor, binding to the *frequency* promoter. *Science.* 297:815–819. doi:10.1126/science.1073681.
20. Yu, Y., W. Dong, C. Altimus, X. Tang, J. Griffith, M. Morello, L. Dudek, J. Arnold, and H. B. Schuttler. 2007. A genetic network for the clock of *Neurospora crassa*. *Proc. Natl. Acad. Sci. USA.* 104:2809–2814. doi:10.1073/pnas.0611005104.
21. Radhakrishnan, K., and A. C. Hindmarsh. 1993. Description and Use of LSODE, the Livermore Solver for Ordinary Differential Equations, Cleveland, OH 44135–3191: National Aeronautics and Space Administration, Lewis Research Center. Report nr NASA Reference Publication 1327.
22. Ermentrout, B. 2002. Simulating, Analyzing, and Animating Dynamical Systems. Siam, Philadelphia.
23. Aronson, B. D., K. A. Johnson, J. J. Loros, and J. C. Dunlap. 1994. Negative feedback defining a circadian clock: autoregulation of the clock gene *frequency*. *Science.* 263:1578–1584. doi:10.1126/science.8128244.
24. Strogatz, S. H. 2000. Nonlinear Dynamics and Chaos. Da Capo Press, New York.
25. Collett, M. A., J. C. Dunlap, and J. J. Loros. 2001. Circadian clock-specific roles for the light response protein WHITE COLLAR-2. *Mol. Cell. Biol.* 21:2619–2628. doi:10.1128/MCB.21.8.2619-2628.2001.
26. Aronson, B. D., K. A. Johnson, and J. C. Dunlap. 1994. Circadian clock locus frequency: protein encoded by a single open reading frame defines period length and temperature compensation. *Proc. Natl. Acad. Sci. USA.* 91:7683–7687. doi:10.1073/pnas.91.16.7683.
27. Gardner, G. F., and J. F. Feldman. 1981. Temperature compensation of circadian periodicity in clock mutants of *Neurospora crassa*. *Plant Physiol.* 68:1244–1248.
28. Ruoff, P., S. Mohsenzadeh, and L. Rensing. 1996. Circadian rhythms and protein turnover: the effect of temperature on the period lengths of clock mutants simulated by the Goodwin oscillator. *Naturwissenschaften.* 83:514–517. doi:10.1007/BF01141953.
29. Ruoff, P., M. Vinsjevik, C. Monnerjahn, and L. Rensing. 1999. The Goodwin oscillator: on the importance of degradation reactions in the circadian clock. *J. Biol. Rhythms.* 14:469–479. doi:10.1177/074873099129001037.
30. Liu, Y., J. Loros, and J. C. Dunlap. 2000. Phosphorylation of the *Neurospora* clock protein FREQUENCY determines its degradation rate and strongly influences the period length of the circadian clock. *Proc. Natl. Acad. Sci. USA.* 97:234–239. doi:10.1073/pnas.97.1.234.
31. Ruoff, P., J. J. Loros, and J. C. Dunlap. 2005. The relationship between FRQ-protein stability and temperature compensation in the *Neurospora* circadian clock. *Proc. Natl. Acad. Sci. USA.* 102:17681–17686. doi:10.1073/pnas.0505137102.
32. Gorl, M., M. Merrow, B. Huttner, J. Johnson, T. Roenneberg, and M. Brunner. 2001. A PEST-like element in FREQUENCY determines the length of the circadian period in *Neurospora crassa*. *EMBO J.* 20:7074–7084. doi:10.1093/emboj/20.24.7074.
33. Liu, Y., M. Merrow, J. J. Loros, and J. C. Dunlap. 1998. How temperature changes reset a circadian oscillator. *Science.* 281:825–829. doi:10.1126/science.281.5378.825.
34. He, Q., J. Cha, Q. He, H. C. Lee, Y. Yang, and Y. Liu. 2006. CKI and CKII mediate the FREQUENCY-dependent phosphorylation of the WHITE COLLAR complex to close the *Neurospora* circadian negative feedback loop. *Genes Dev.* 20:2552–2565. doi:10.1101/gad.1463506.
35. Goodwin, B. C. 1965. Oscillatory behavior in enzymatic control processes. *Adv. Enzyme Regul.* 3:425–438. doi:10.1016/0065-2571(65)90067-1.
36. Ruoff, P., and L. Rensing. 1996. The temperature-compensated Goodwin model simulates many circadian clock properties. *J. Theor. Biol.* 179:275–285. doi:10.1006/jtbi.1996.0067.
37. He, Q., and Y. Liu. 2005. Degradation of the *Neurospora* circadian clock protein FREQUENCY through the ubiquitin-proteasome pathway. *Biochem. Soc. Trans.* 33:953–956. doi:10.1042/BST20050953.
38. Thomas, M. C., and C. M. Chiang. 2006. The general transcription machinery and general cofactors. *Crit. Rev. Biochem. Mol. Biol.* 41:105–178. doi:10.1080/10409230600648736.
39. Hochachka, P. W., and G. N. Somero. 2002. Biochemical Adaptation. Mechanism and Process in Physiological Evolution. Oxford University Press, Oxford.
40. Londesborough, J. 1980. The causes of sharply bent or discontinuous Arrhenius plots for enzyme-catalysed reactions. *Eur. J. Biochem.* 105:211–215. doi:10.1111/j.1432-1033.1980.tb04491.x.
41. Marjanovic, M., D. Zivadinovic, Z. Dzakula, and R. K. Andjus. 2005. Mechanisms of immediate temperature compensation: experiments with brain synaptosomes from rat and ground squirrel. *Ann. N. Y. Acad. Sci.* 1048:47–59. doi:10.1196/annals.1342.005.
42. Peracchi, A. 1999. Origins of the temperature dependence of hammerhead ribozyme catalysis. *Nucleic Acids Res.* 27:2875–2882. doi:10.1093/nar/27.14.2875.
43. Ruoff, P. 1992. Introducing temperature-compensation in any reaction kinetic oscillator model. *J. Interdiscipl. Cycle Res.* 23:92–99.
44. Hastings, J. W., and B. M. Sweeney. 1957. On the mechanism of temperature independence in a biological clock. *Proc. Natl. Acad. Sci. USA.* 43:804–811. doi:10.1073/pnas.43.9.804.
45. Kovacs, K., L. L. Hussami, and G. Rabai. 2005. Temperature compensation in the oscillatory bray reaction. *J. Phys. Chem. A.* 109:10302–10306.
46. Kóvacs, K. M., and G. Rábai. 2002. Temperature-compensation in pH-oscillators. *Phys. Chem. Chem. Phys.* 4:5265–5269. doi:10.1039/b206497a.

47. Rábai, G., and I. Hanazaki. 1999. Temperature compensation in the oscillatory hydrogen peroxide-thiosulfate-sulfite flow system. *Chem. Commun.* 1965–1966. doi:10.1039/a906598i.

48. Ruoff, P. 1995. Antagonistic balance in the Oregonator: about the possibility of temperature-compensation in the Belousov-Zhabotinsky reaction. *Physica D*. 84:204–211. doi:10.1016/0167-2789(95)00018-Y.

49. Ruoff, P., M. K. Christensen, J. Wolf, and R. Heinrich. 2003. Temperature dependency and temperature-compensation in a model of yeast glycolytic oscillations. *Biophys. Chem.* 106:179–192. doi:10.1016/S0301-4622(03)00191-1.

50. Valeur, K. R., and R. degli Agosti. 2002. Simulations of temperature sensitivity of the peroxidase-oxidase oscillator. *Biophys. Chem.* 99: 259–270. doi:10.1016/S0301-4622(02)00226-0.

51. Eckardt, N. A. 2006. A wheel within a wheel: temperature compensation of the circadian clock. *Plant Cell.* 18:1105–1108. doi:10.1105/tpc.106.043356.

52. Edwards, K. D., J. R. Lynn, P. Gyula, F. Nagy, and A. J. Millar. 2005. Natural allelic variation in the temperature compensation mechanisms of the *Arabidopsis thaliana* circadian clock. *Genetics.* 170:387–400. doi:10.1534/genetics.104.035238.

53. Gould, P. D., J. C. Locke, C. Larue, M. M. Southern, S. J. Davis, S. Hanano, R. Moyle, R. Milich, J. Putterill, A. J. Millar, and A. Hall. 2006. The molecular basis of temperature compensation in the *Arabidopsis* circadian clock. *Plant Cell.* 18:1177–1187. doi:10.1105/tpc.105.039990.

54. Locke, J. C., M. M. Southern, L. Kozma-Bognar, V. Hibberd, P. E. Brown, M. S. Turner, and A. J. Millar. 2005. Extension of a genetic network model by iterative experimentation and mathematical analysis. *Mol. Syst. Biol.* 1:2005 0013.

55. Ruoff, P., M. Zakhartsev, and H. V. Westerhoff. 2007. Temperature compensation through systems biology. *FEBS J.* 274:940–950. doi:10.1111/j.1742-4658.2007.05641.x.

56. Hong, C. I., E. D. Conrad, and J. J. Tyson. 2007. A proposal for robust temperature compensation of circadian rhythms. *Proc. Natl. Acad. Sci. USA.* 104:1195–1200. doi:10.1073/pnas.0601378104.

57. Kurosawa, G., and Y. Iwasa. 2005. Temperature compensation in circadian clock models. *J. Theor. Biol.* 233:453–468. doi:10.1016/j.jtbi.2004.10.012.

58. Ruoff, P., M. Vinsjevik, and L. Rensing. 2000. Temperature compensation in biological oscillators: a challenge for joint experimental and theoretical analysis. *Comments Theor. Biol.* 5: 361–382.

59. Smolen, P., P. E. Hardin, B. S. Lo, D. A. Baxter, and J. H. Byrne. 2004. Simulation of *Drosophila* circadian oscillations, mutations, and light responses by a model with VRI, PDP-1, and CLK. *Biophys. J.* 86: 2786–2802.

60. Lakin-Thomas, P. L., S. Brody, and G. G. Cote. 1991. Amplitude model for the effects of mutations and temperature on period and phase resetting of the *Neurospora* circadian oscillator. *J. Biol. Rhythms.* 6:281–297. doi:10.1177/074873049100600401.

61. Winfree, A. T. 2000. The geometry of biological time, 2nd ed. Springer-Verlag, New York.

62. Gonze, D., J. C. Leloup, and A. Goldbeter. 2000. Theoretical models for circadian rhythms in *Neurospora* and *Drosophila*. *C. R. Acad. Sci. III.* 323:57–67.

63. Leloup, J. C., D. Gonze, and A. Goldbeter. 1999. Limit cycle models for circadian rhythms based on transcriptional regulation in *Drosophila* and *Neurospora*. *J. Biol. Rhythms.* 14:433–448. doi:10.1177/074873099129000948.

64. Ruoff, P., M. Vinsjevik, S. Mohsenzadeh, and L. Rensing. 1999. The Goodwin model: simulating the effect of cycloheximide and heat shock on the sporulation rhythm of *Neurospora crassa*. *J. Theor. Biol.* 196: 483–494. doi:10.1006/jtbi.1998.0846.

65. Ruoff, P., M. Vinsjevik, C. Monnerjahn, and L. Rensing. 2001. The Goodwin model: simulating the effect of light pulses on the circadian sporulation rhythm of *Neurospora crassa*. *J. Theor. Biol.* 209:29–42. doi:10.1006/jtbi.2000.2239.

66. Smolen, P., D. A. Baxter, and J. H. Byrne. 2003. Reduced models of the circadian oscillators in *Neurospora crassa* and *Drosophila melanogaster* illustrate mechanistic similarities. *OMICS.* 7:337–354. doi:10.1089/153623103322637661.

67. Francois, P. 2005. A model for the *Neurospora* circadian clock. *Biophys. J.* 88:2369–2383. doi:10.1529/biophysj.104.053975.

68. Sriram, K., and M. S. Gopinathan. 2004. A two variable delay model for the circadian rhythm of *Neurospora crassa*. *J. Theor. Biol.* 231:23–38. doi:10.1016/j.jtbi.2004.04.006.

69. Smolen, P., D. A. Baxter, and J. H. Byrne. 2001. Modeling circadian oscillations with interlocking positive and negative feedback loops. *J. Neurosci.* 21:6644–6656.